

AD _____

Award Number: DAMD17-00-1-0318

TITLE: Markers of Increased Risk in Pre-Invasive Breast Cancer

PRINCIPAL INVESTIGATOR: Adewale Adeyinka, Ph.D.
Soma Mandel, Ph.D.
Peter Watson, Ph.D.

CONTRACTING ORGANIZATION: University of Manitoba
Winnipeg, Manitoba R3E 0W3 Canada

REPORT DATE: February 2003

TYPE OF REPORT: Annual Summary

PREPARED FOR: U.S. Army Medical Research and Materiel Command
Fort Detrick, Maryland 21702-5012

DISTRIBUTION STATEMENT: Approved for Public Release;
Distribution Unlimited

The views, opinions and/or findings contained in this report are those of the author(s) and should not be construed as an official Department of the Army position, policy or decision unless so designated by other documentation.

20030416 248

REPORT DOCUMENTATION PAGE

Form Approved
OMB No. 074-0188

Public reporting burden for this collection of information is estimated to average 1 hour per response, including the time for reviewing instructions, searching existing data sources, gathering and maintaining the data needed, and completing and reviewing this collection of information. Send comments regarding this burden estimate or any other aspect of this collection of information, including suggestions for reducing this burden to Washington Headquarters Services, Directorate for Information Operations and Reports, 1215 Jefferson Davis Highway, Suite 1204, Arlington, VA 22202-4302, and to the Office of Management and Budget, Paperwork Reduction Project (0704-0188), Washington, DC 20503

1. AGENCY USE ONLY (Leave blank)			2. REPORT DATE February 2003	3. REPORT TYPE AND DATES COVERED Annual Summary (1 Jan 02 - 1 Jan 03)
4. TITLE AND SUBTITLE Markers of Increased Risk in Pre-Invasive Breast Cancer			5. FUNDING NUMBERS DAMD17-00-1-0318	
6. AUTHOR(S) Adewale Adeyinka, Ph.D. Soma Mandel, Ph.D. Peter Watson, Ph.D.				
7. PERFORMING ORGANIZATION NAME(S) AND ADDRESS(ES) University of Manitoba Winnipeg, Manitoba R3E 0W3 Canada E-Mail: adeyinka@cc.umanitoba.ca			8. PERFORMING ORGANIZATION REPORT NUMBER	
9. SPONSORING / MONITORING AGENCY NAME(S) AND ADDRESS(ES) U.S. Army Medical Research and Materiel Command Fort Detrick, Maryland 21702-5012			10. SPONSORING / MONITORING AGENCY REPORT NUMBER	
11. SUPPLEMENTARY NOTES				
12a. DISTRIBUTION / AVAILABILITY STATEMENT Approved for Public Release; Distribution Unlimited				12b. DISTRIBUTION CODE
13. Abstract (Maximum 200 Words) (abstract should contain no proprietary or confidential information) The risk of recurrence and progression of ductal carcinoma in-situ (DCIS) of the breast is best designated by morphological indicators including the presence of necrosis. To identify molecular alterations underlying this morphological feature we have compared gene expression within a cohort of 6 cases of DCIS with necrosis (DCIS ^{necrosis+}) and 4 cases without necrosis (DCIS ^{necrosis-}) using microdissection and cDNA microarray. A set of 69 cDNAs, from a group of 1,181, was identified that were consistently differentially expressed. Amongst this set, the mRNA for angio-associated migratory cell protein (AAMP) and a serine threonine protein kinase, nuclear Dbf2 related (NDR), were consistently higher in DCIS ^{necrosis+} and were also found to be overexpressed in the T47D breast cancer cell line subjected to hypoxia. A significant differential expression (P=0.0095) was confirmed for AAMP by quantitative reverse transcriptase polymerase chain reaction (RT-PCR). Further study of AAMP by RT-PCR and in situ hybridization analysis of 37 cases of DCIS also confirmed that a higher AAMP mRNA expression tended to be associated with high-grade nuclear morphology and necrosis. The present study shows that while levels of gene expression are mostly similar between morphologically different DCIS, consistent differences in expression of a subset of genes can be identified between DCIS with and without necrosis.				
14. SUBJECT TERMS: breast cancer, DCIS, gene expression profile				15. NUMBER OF PAGES 22
				16. PRICE CODE
17. SECURITY CLASSIFICATION OF REPORT Unclassified	18. SECURITY CLASSIFICATION OF THIS PAGE Unclassified	19. SECURITY CLASSIFICATION OF ABSTRACT Unclassified	20. LIMITATION OF ABSTRACT Unlimited	

Table of Contents

Cover.....	1
SF 298.....	2
Introduction.....	3
Body.....	5
Key Research Accomplishments.....	8
Reportable Outcomes.....	9
Conclusions.....	9
References.....	10
Appendices.....	11

INTRODUCTION

In recent years there has been an increase in the numbers of ductal carcinoma in-situ (DCIS) and other pre-invasive breast lesions diagnosed (1, 2). As a result, these lesions have become an increasingly significant problem in the evaluation and management of patients with breast disease. To predict the relative risk of recurrence and/or the progression of DCIS to invasive tumors, different classifications have been proposed(3). These are based on a combination of morphological features such as nuclear grade, presence of necrosis, margin width and tumor size, and reflect a recognition that DCIS is in fact a spectrum of disease with different morphological characteristics as well as biological and clinical behavior. However, useful as these classifications may be, discordance is common in their use (4) and the risk of recurrence varies within

categories, underscoring the need for better predictors of outcome and progression of DCIS. Although DCIS lesions are common (now accounting for 10-15% of all new breast cancer cases), the small average size (5, 6) and the requirement to submit entire specimens suspected of harboring DCIS lesions for microscopic examination (7), severely limits the number of samples available as frozen tissue for RNA and gene expression studies to identify such predictors. However, drawing on a mature frozen tissue tumor bank resource (8), and combining manual and laser capture microdissection (LCM) methods (9,10) with cDNA microarray analysis, we sought to identify genes activated in higher risk DCIS compared to lower risk DCIS. As already noted, intraductal necrosis is a distinctive morphological feature of some types of high risk DCIS (11) and is believed to be attributable to the presence of severe hypoxia that can arise within the duct through an imbalance between metabolic requirements and blood supply (12). We therefore compared regions of DCIS associated with intraductal necrosis with regions of DCIS not associated with intraductal necrosis. We assumed that amongst the genes that we would find to be overexpressed in high risk DCIS would be some that were induced directly by hypoxia and some associated with the chronic downstream ramifications of the hypoxic response, such as cell metabolic changes. But also recognizing that some genes might be unrelated to hypoxia as not all necrosis may be attributable to hypoxia. It is anticipated that some of the products of those genes identified may serve as molecular biomarkers of biological status and cellular stress in DCIS and thus have potential for assessing the risk of progression or providing targets for new therapies.

Objectives:

The overall aim of the study is to identify genetic molecular markers of the risk of recurrence of in-situ breast lesions. The specific aims are:

Specific aim 1. To identify and clone genes that are differentially expressed between high and low grade DCIS that may contribute to their known risks of recurrence.

Specific aim 2. To study the role of candidate genes identified in specific aim 1 by assessment of expression in-vivo and by manipulations of expression in breast cell lines.

BODY OF REPORT

Accomplishments in the context of the specific aims defined in the statement of work

Specific aim 1.

Four high grade and 2 intermediate grade DCIS with necrosis (DCIS ^{necrosis+}), and 4 low-grade human DCIS samples (DCIS^{necrosis-}), with homogeneous nuclear grade within each lesion, were obtained from the NCIC-Manitoba Breast Tumor Bank (Department of Pathology, University of Manitoba, Winnipeg, Canada) for microdissection. Tumor samples were microdissected by two methods — a rapid and reliable manual dissection-microscope method previously established in our laboratory and a laser-capture microdissection method using an Arcturus Pixell II instrument (Arcturus Engineering, Inc.

Mountain View, CA) depending on the size and the geographical complexity of the DCIS lesions.

³³P-labeled reversed transcribed total RNA extracted from microdissected tumor cells was hybridized to the GF200 Human Gene Filters (Research Genetics) containing 5,184 spotted cDNAs. Tiff images representing the gene expression pattern for each tumor sample were obtained using a phosphorimager. The 6 DCIS with necrosis were compared to the 4 DCIS without necrosis using the Pathways 3.0 software. The Chen and t tests were applied using the Pathways 3.0 software (at a confidence level of 75%) to filter out cDNA pairs (4,363 or 78% of the 5,544 transcripts represented on the membrane) whose mean intensities were not statistically different. Of the remaining 1181 transcripts, we masked those with intensities lower than 5x background and excluded false positives; spots judged to be influenced by "bleed over" from adjacent spots. After this filtering process 69 transcripts remained that were 1.5 fold or more differentially expressed between the six DCIS^{necrosis+} and 4 DCIS^{necrosis-}. Fifty-two of the transcripts were overexpressed by the DCIS^{necrosis+} group and 17 transcripts were overexpressed by the DCIS^{necrosis-} group. A similar approach was used to compare profiles of gene expression between normoxic and hypoxic T47D breast cells.

The Pathways 3.0 software is an improvement on the Pathways 2.01 software used in the data presented in the January 1, 2001-January 1, 2002 annual report. The reanalysis of our data using the pathways 3.0 software enabled us to use a more robust statistical approach to identify differentially expressed genes. (See Appendix 3 for details and figures)

Specific aim 2

Intraductal necrosis is a distinctive morphological feature of some types of high risk DCIS (8), molecular mechanisms associated with the hypoxia response or activation of the normal response to less severe hypoxia may therefore offer potential indicators of risk of progression in DCIS lesions. To identify genes that were both differentially expressed and that also might be associated with hypoxia, we compared the set of 52 cDNAs consistently overexpressed in high-grade DCIS with 22 cDNAs found to be overexpressed in the T47D cell line subjected to hypoxia, and analyzed in parallel with the DCIS lesions using the same microarray filter. The angio associated migratory protein (AAMP) and nuclear Dbf2 related (NDR) genes were found to be common to both sets of differentially expressed transcripts. They were further assessed by real time quantitative RT-PCR on RNA extracted from the 10 microdissected samples and 28 more DCIS lesions (not microdissected) selected from our Tumor Bank and by in situ hybridization studies (AAMP only) on paraffin-embedded sections from these tumors. Differential expression of the mRNA for AAMP was confirmed by both methods, albeit to different significant levels by RT-PCR among the microdissected tumors and the non-microdissected tumors (see details and figures in Appendix 3).

KEY RESEARCH ACCOMPLISHMENTS

- Identify, using microdissection techniques and cDNA microarray analysis, a subset of genes consistently differentially expressed between DCIS with necrosis and DCIS without necrosis.
- Demonstrate by a combination of cDNA array analysis, real time RT-PCR, and *in-situ* hybridization that expression of the mRNA for angio associated migratory protein, previously shown to be associated with angiogenesis and tumor progression (13, 14), is associated with a high-grade nuclear morphology and necrosis in DCIS lesions of the breast.
- Demonstrate by a combination of cDNA array analysis and real time RT-PCR that expression of the mRNA for nuclear Dbf2 related (NDR) is associated with a high-grade nuclear morphology and necrosis in DCIS lesions of the breast.

REPORTABLE OUTCOMES

Abstract

1. Adewale Adeyinka, Ethan D. Emberley, Charles C. Wykoff, Adrian Harris, Leigh C. Murphy and Peter H. Watson. DIFFERENTIAL GENE EXPRESSION ANALYSIS OF MICRODISSECTED DUCTAL CARCINOMA *IN SITU* (DCIS) OF THE BREAST. Proceedings of the American Association for Cancer Research. 42: 58, 2001
2. Adewale Adeyinka, Ethan Emberley, Leigh C. Murphy, Heidi Sowter, Charles C. Wykoff, Adrian L. Harris, and Peter H. Watson. ANALYSIS OF GENE EXPRESSION IN PRE-INVASIVE BREAST CANCER. The Department of Defense Breast Cancer Research program Meeting. September 2002

Oral presentation

PRE-INVASIVE BREAST CANCERS (DCIS) ASSOCIATED WITH HIGH-RISK AND LOW-RISK OF RECURRENCE DIFFER IN THEIR PATTERNS OF GENE EXPRESSION. Canadian Breast Cancer Research Initiative, Reasons for Hope. May 2001

Publication

Adewale Adeyinka, Ethan Emberley, Yulian Niu, Linda Snell, Leigh C. Murphy, Heidi Sowter, Charles Wykoff, Adrian L. Harris, and Peter H. Watson. ANALYSIS OF GENE EXPRESSION IN DUCTAL CARCINOMA *IN SITU* OF THE BREAST. Clin Cancer Res. 8: 3788-3795, 2002

CONCLUSIONS

Levels of gene expression are mostly similar between morphologically different DCIS, however, consistent differences in expression of a subset of genes can be identified between DCIS with and without necrosis.

REFERENCES

1. Ernster, V. L., and Barclay, J. Increase in ductal carcinoma *in situ* (DCIS) of breast in relation to mammography: a dilemma. *J. Nat. Cancer Inst. Monogr.*, 22: 151-156, 1997.
2. Elston, C. W., Ellis, I. O., and Pinder, S. E. Prognostic factors in invasive carcinoma of the breast. *Clin Oncol.*, 10: 14-17, 1998.
3. Silverstein, M. J., Lagios, M. D., Craig, P. H., Waisman, J. R., Lewinsky, B. S., Colburn, W. J., and Poller, D. N. A prognostic index for ductal carcinoma *in situ* of the breast. *Cancer*, 77: 2267-2274, 1996.
4. Sneige, N., Lagios, M. D., Schwarting, R., Colburn, W., Atkinson, E., Weber, D., Sahin, A., Kemp, B., Hoque, A., Risin, S., Sabichi, A., Boone, C., Dhingra, K., Kelloff, G., and Lippman, S. Interobserver reproducibility of the Lagios nuclear grading system for ductal carcinoma *in situ*. *Human Pathol.*, 30: 257-262, 1999.
5. Lagios M. D. Duct carcinoma *in situ*: biological implications for clinical practice. *Sem. Oncol.*, 23(suppl I2): 6-11, 1996.
6. Sakorafas G. H., and Tsiotou A. G. H. Ductal carcinoma *in situ* (DCIS) of the breast: evolving perspectives. *Cancer Treat. Rev.*, 26: 103-125, 2000.
7. Winchester D.P., and Strom E. A. Standards for diagnosis and management of ductal carcinoma *in situ* (DCIS) of the breast. *CA Cancer J. Clin.*, 48: 108-128, 1998.
8. Watson, P., Snell, L., and Parisien, M. The role of a tumor bank in translational research. *Canadian Medical Association Journal*, 15: 281-283, 1996.
9. Hiller, T., Snell, L., and Watson, P. H. An approach for microdissection/RT-PCR analysis of gene expression in pathologically defined frozen tissue sections. *Biotechniques*, 21: 38-42, 1996.
10. Luzzi, V., Holtschlag, V., and Watson, M. A. Expression profiling of ductal carcinoma *in situ* by laser capture microdissection and high-density oligonucleotide arrays. *Am. J. Pathol.*, 158: 2005-2010, 2001.
11. Fisher, E. R., Dignam, J., Tan-Chiu, E., Costantino, J., Fisher, B., Paik, S., and Wolmark, N. Pathologic findings from the National Surgical Adjuvant Breast Project (NSABP) eight-year update of Protocol B-17: intraductal carcinoma. *Cancer*, 86: 429-438, 1999.
12. Wykoff, C. C., Beasley, N., Watson, P. H., Campo, L., Chia, S. K., English, R., Pastorek, J., Sly, W. S., Ratcliffe, P., and Harris, A. L. Expression of hypoxia-inducible and tumorassociated carbonic anhydrase in ductal carcinoma *in situ* of the breast. *Am. J. Pathol.*, 158: 1011-1019, 2001.
13. Beckner, M. E., Krutzsch, H. C., Stracke, M. L., Williams, S. T., Gallardo, J. A., and Liotta L. A. Identification of a new immunoglobulin superfamily protein expressed in blood vessels with a heparin-binding consensus sequence. *Cancer Res.*, 55:2140-2149, 1995.
14. Beckner, M. E., and Liotta, L. A. AAMP, a conserved protein with immunoglobulin and WD40 domains, regulates endothelial tube formation *in vitro*. *Lab Invest.*, 75: 97-107, 1996.



American Association for Cancer Research

92nd
Annual Meeting

March 24-28, 2001 • New Orleans, LA

Volume 42 • March 2001

Proceedings

#310 Differential Gene Expression Analysis of Microdissected Ductal Carcinoma in Situ (DCIS) of the Breast. Adewale Adeyinka, Ethan D. Emberley, Charles C. Wykoff, Adrian L. Harris, Leigh C. Murphy, and Peter H. Watson. *John Radcliffe Hospital, Oxford, UK, and University of Manitoba, Winnipeg, MB, Canada.*

In situ breast carcinomas are now recognized as a spectrum of diseases with different morphology, biological and clinical behavior. We hypothesize a molecular/genetic basis for these differences and have, therefore, compared the gene expression profile, using cDNA microarray membranes, of 4 high-grade and 6 non-high-grade (Van Nuys classification system) microdissected ductal carcinoma in situ of the breast. Tumors for analysis were obtained from the NCIC Manitoba breast tumor bank. ^{33}P -labeled total RNA from tumors were hybridized to GF200 Human Gene Filters (Research Genetics) containing 5,184 spotted cDNAs. Analysis of our data, employing the Pathways 2.01 analysis software (Research Genetics), showed that an average of 61 (S.D. = 40) cDNAs were over expressed (greater than or equal to 1.8 fold difference in expression) in high-grade tumors compared with non-high-grade tumors. Amongst these sequences, at least 33 cDNAs were found to be over expressed in three or more pairs of high-grade vs low grade tumors and a small subset of these sequences were also found to be overexpressed in breast cell lines subjected to hypoxia. These findings show that there are consistent differences in the gene expression pattern of high-grade and non-high-grade in situ breast tumors. Some of these differentially expressed genes may play an important role in determining the biologic and clinical behavior of these tumors and further study is warranted to confirm the differential expression of these genes at the protein level and to determine their relevance in breast cancer progression.

End Of Hope

Department of Defense
Breast Cancer Research
Program Meeting

October 25-28, 2002

Proceedings

ANALYSIS OF GENE EXPRESSION IN
PRE-INVASIVE BREAST CANCER

Adewale Adeyinka,² Ethan Emberley,²
Leigh C. Murphy,² Heidi Sowter,¹ Charles C. Wykoff,¹
Adrian L. Harris,¹ and Peter H. Watson²

¹John Radcliffe Hospital, Oxford, OX3 9DU, UK; and
²University of Manitoba, Winnipeg, Manitoba, R3E 0W3 Canada

adeyinka@cc.umanitoba.ca

In recent years there has been an increase in the numbers of ductal carcinoma *in situ* (DCIS) and other pre-invasive breast lesions diagnosed. As a result, these lesions have become an increasingly significant problem in the evaluation and management of patients with breast disease. The risk of recurrence and progression of ductal carcinoma *in situ* (DCIS) of the breast is best designated by morphological indicators including the presence of necrosis. To identify molecular alterations underlying this morphological feature we have compared gene expression within a cohort of 6 cases of DCIS with necrosis (DCISnecrosis+) and 4 cases without necrosis (DCISnecrosis-) using microdissection and cDNA microarray. A set of 69 cDNAs, from a group of 1,181, was identified that were consistently differentially expressed. Amongst this set, the mRNA for angio-associated migratory cell protein (AAMP) and a serine threonine protein kinase, NDR, were consistently higher in DCISnecrosis+ and were also found to be overexpressed in the T47D breast cancer cell line subjected to hypoxia. Differential expression of both genes was confirmed by quantitative reverse transcriptase polymerase chain reaction (RT-PCR), particularly for AAMP ($P=0.0095$). Further study of AAMP by RT-PCR and *in situ* hybridization analysis of 37 cases of DCIS also confirmed that a higher AAMP mRNA expression tended to be associated with high- and intermediate-grade nuclear morphology and the presence of necrosis. The present study shows that while levels of gene expression are mostly similar between morphologically different DCIS, consistent differences in expression of a subset of genes can be identified between DCIS with and without necrosis. It is anticipated that some of the products of the differentially expressed genes may serve as molecular biomarkers for assessing the risk of progression of DCIS.

Analysis of Gene Expression in Ductal Carcinoma *in Situ* of the Breast¹

Adewale Adeyinka, Ethan Emberley, Yulian Niu, Linda Snell, Leigh C. Murphy, Heidi Sowter, Charles C. Wykoff, Adrian L. Harris, and Peter H. Watson²

Departments of Pathology [A. A., E. E., Y. N., L. S., P. H. W.] and Biochemistry and Molecular Biology [L. C. M.], University of Manitoba, Faculty of Medicine, Winnipeg, Manitoba, R3E 0W3 Canada, and Cancer Research United Kingdom Molecular Oncology Laboratory, University of Oxford, Institute of Molecular Medicine, John Radcliffe Hospital, Oxford OX3 9DU, United Kingdom [H. S., C. C. W., A. L. H.]

ABSTRACT

Purpose: The risk of recurrence and progression of ductal carcinoma *in situ* (DCIS) of the breast is best designated by morphological indicators, including the presence of necrosis. Our purpose was to identify molecular alterations underlying progression of DCIS.

Experimental Design: We have compared gene expression within a cohort of six cases of DCIS with necrosis (DCIS^{necrosis+}) and four cases without necrosis (DCIS^{necrosis-}) using microdissection and cDNA microarray.

Results: A set of 69 cDNAs from a group of 1181 was identified that were consistently differentially expressed. Among this set, the mRNA for angio-associated migratory cell protein and a serine threonine protein kinase, nuclear Dbf2 related, were consistently higher in DCIS^{necrosis+} and were also found to be overexpressed in the T47D breast cancer cell line subjected to hypoxia. Further study of angio-associated migratory cell protein by quantitative reverse transcriptase-PCR and *in situ* hybridization analysis of 37 cases of DCIS confirmed higher mRNA expression in DCIS^{necrosis+} ($P = 0.0095$).

Conclusions: This study shows that although levels of gene expression are mostly similar between morphologically

different DCIS, consistent differences in expression of a subset of genes can be identified between DCIS with and without necrosis.

INTRODUCTION

In recent years, there has been an increase in the numbers of DCIS³ and other preinvasive breast lesions diagnosed (1, 2). As a result, these lesions have become an increasingly significant problem in the evaluation and management of patients with breast disease. To predict the relative risk of recurrence and/or the progression of DCIS to invasive tumors, different classifications have been proposed (3). These are based on a combination of morphological features such as nuclear grade, presence of necrosis, margin width, and tumor size and reflect a recognition that DCIS is in fact a spectrum of disease with different morphological characteristics as well as biological and clinical behavior. However, useful as these classifications may be, discordance is common in their use (4) and the risk of recurrence varies within categories, underscoring the need for better predictors of outcome and progression of DCIS.

Although DCIS lesions are common (now accounting for 10–15% of all new breast cancer cases), the small average size (5, 6) and the requirement to submit entire specimens suspected of harboring DCIS lesions for microscopic examination (7) severely limits the number of samples available as frozen tissue for RNA and gene expression studies to identify such predictors. However, drawing on a mature frozen tissue tumor bank resource (8) and combining manual and LCM methods (9, 10) with cDNA microarray analysis, we sought to identify genes activated in higher risk DCIS compared with lower risk DCIS. As already noted, intraductal necrosis is a distinctive morphological feature of some types of high risk DCIS (11) and is believed to be attributable to the presence of severe hypoxia that can arise within the duct through an imbalance between metabolic requirements and blood supply (12). We therefore compared regions of DCIS associated with intraductal necrosis with regions of DCIS not associated with intraductal necrosis. We assumed that among the genes that we would find to be overexpressed in high-risk DCIS would be some that were induced directly by hypoxia and some associated with the chronic downstream ramifications of the hypoxic response such as cell metabolic changes. However, also recognizing that some overexpressed genes might be unrelated to hypoxia as not all necrosis may be attributable to hypoxia. It is anticipated that some of the products of those genes identified may serve as molecular

Received 3/11/02; revised 8/19/02; accepted 8/20/02.

The costs of publication of this article were defrayed in part by the payment of page charges. This article must therefore be hereby marked *advertisement* in accordance with 18 U.S.C. Section 1734 solely to indicate this fact.

¹ This work was supported, in part, by grants from the Canadian Institutes of Health (CIHR), the Canadian Breast Cancer Research Initiative, and the United States Army Medical Research and Materiel Command (USAMRMC). The Manitoba Breast Tumor Bank is supported by funding from the National Cancer Institute of Canada. E. E. is supported by a USAMRMC predoctoral award. A. A. is supported by a USAMRMC postdoctoral award. P. H. W. is supported by a CIHR Scientist award and by a USAMRMC Academic Award.

² To whom requests for reprints should be addressed, at Department of Pathology, D212-770 Bannatyne Avenue, University of Manitoba, Winnipeg, Manitoba R3E 0W3, Canada. Phone: (204) 789-3435; Fax: (204) 789-3931; E-mail: pwatson@cc.umanitoba.ca.

³ The abbreviations used are: DCIS, ductal carcinoma *in situ*; LCM, laser capture microdissection; AAMP, angio-associated migratory cell protein; NDR, nuclear Dbf2 related; RT-PCR, reverse transcription-polymerase chain reaction; ER, estrogen receptor; PR, progesterone receptor; ISH, *in situ* hybridization; CA, carbonic anhydrase.

biomarkers of biological status and cellular stress in DCIS and thus have potential for assessing the risk of progression or providing targets for new therapies.

MATERIALS AND METHODS

Human Breast Tumor Samples. Human DCIS samples were obtained from the Manitoba Breast Tumor Bank (Department of Pathology, University of Manitoba, Winnipeg, Canada; Ref. 8). All cases in the bank have been rapidly frozen at 70°C after surgical removal and subsequently processed to create formalin-fixed, paraffin-embedded tissue blocks and matched frozen tissue blocks with mirror image surfaces corresponding to the formalin-fixed tissue blocks (9). Histological interpretation and assessment of every sample in the Bank is done on H&E-stained sections from the paraffin tissue by a pathologist.

Two cohorts of tumors were selected. The first cohort of 10 tumors were selected to include only DCIS with homogenous nuclear grade throughout and comprised 6 DCIS with necrosis (4 high nuclear grade, 2 intermediate nuclear grade), and 4 DCIS without necrosis (all 4 low nuclear grade). These cases were used as the primary microdissection series. The second cohort comprised 28 DCIS cases with heterogeneous nuclear grade that were used to confirm the differential expression observed in the microdissected cases. Tumor classification and the evaluation of intraductal necrosis were done on high-quality H&E-stained slides derived from the formalin-fixed and paraffin-embedded blocks independent of the array or subsequent gene expression analysis. Additional classification of DCIS into histological grades was done according to the Van Nuys pathological classification (13), and tumors in the second cohort were assigned to the highest histological grade present in the tissue section studied. Both cohorts combined (38 tumors) included 17 low and intermediate grade DCIS (nonhigh grade DCIS, including 7 with necrosis and 10 without necrosis) and 21 high-grade DCIS. Twenty-seven tumors were ER-positive, 11 were ER-negative, 25 were PR-positive and 13 were PR-negative (Table 1). Steroid receptor status was determined by ligand-binding assay. A positive ER status and positive PR status were defined as >3 fmol/mg protein and >15 fmol/mg protein, respectively.

Tissue Microdissection and RNA Extraction. Tumor samples were microdissected by two methods, depending on the size and the geographical complexity of the DCIS lesions. A manual dissection microscope method previously established in our laboratory (9) was used where possible as it is rapid and reliable; however, a LCM method using an Arcturus Pixell II instrument (Arcturus Engineering, Inc., Mountain View, CA) was used for two cases with a heavy inflammatory cell infiltrate of the stroma around the ducts. For the manual microdissection, tumor cells were dissected from 6 to 10 20- μ m each frozen sections from each tumor and mounted on agarose gel, dropped onto a plain glass slide, and stained briefly with H&E, as described previously (9). For laser microdissection, tumor cells were microdissected from 14 to 17 10- μ m frozen sections mounted onto plain glass slides and stained with H&E according to the protocol recommended by Arcturus Engineering, Inc. The nature of the tissue processing, with matching mirror image paraffin and frozen blocks (9), ensured that we could determine that all areas microdissected were of high and comparable

Table 1 Morphology, steroid receptor status, and AAMP expression of 37 DCIS of the breast

Serial no. ^a	Case no.	Nuclear grade ^b	Necrosis	ER status ^c	PR status ^d	AAMP RT-PCR ^e
1	12024	HG	+	—	—	0.21
2	10046	HG	+	—	—	0.13
3	13110	HG	+	+	—	0.34
4	13049	HG	+	+	+	0.31
5	11970	IG	+	—	—	0.31
6	11722	IG	+	+	+	0.11
7	10047	LG	—	+	+	0.1
8	11161	LG	—	+	+	0.09
9	9062	LG	—	+	+	0.1
10	10919	LG	—	+	+	0.11
11	12340	HG	+	—	—	1.3
12	13115	HG	+	—	+	0.63
13	15200	HG	+	+	—	1.03
14	11972	HG	+	—	—	0.53
15	12054	HG	+	—	—	0.56
16	12485	HG	+	+	—	0.39
17	15242	HG	+	—	+	0.37
18	11202	HG	+	+	+	0.72
19	12354	HG	+	+	+	0.34
20	13523	HG	+	+	+	0.39
21	13423	HG	+	+	—	0.34
22	12338	HG	+	+	+	1.08
23	14815	HG	+	+	+	0.58
24	15134	HG	+	+	+	0.49
25	13005	HG	+	—	—	0.46
26	11442	HG	—	+	+	1.33
27	15344	IG	+	+	+	0.55
28	11285	IG	+	+	—	0.72
29	14902	IG	+	—	+	0.74
30	15108	IG	+	+	+	0.46
31	15010	IG	+	+	+	1.22
32	10351	IG	—	+	+	0.38
33	15439	IG	—	+	+	0.32
34	12438	IG	—	—	—	0.64
35	12571	IG	—	+	+	0.44
36	13686	LG	—	+	+	0.44
37	15284	LG	—	+	+	0.47

^a Serial #1–10 = cohort #1, microdissected tumors. #11–37 = cohort #2.

^b HG = high-grade; IG = intermediate-grade; LG = low-grade.

^c ER less than 3.0 fmol/mg protein = —; ER more than 3.0 fmol/mg protein = +.

^d PR less than 15.0 fmol/mg protein = —; PR more than 15.0 fmol/mg protein = +.

^e AAMP RT-PCR = AAMP mRNA level (arbitrary units) measured by RT-PCR relative to a control gene (cyclophilin).

quality viable tissue, and care was taken to avoid inclusion of intraluminal necrotic material.

Total RNA was extracted with Trizol Reagent (Life Technologies, Inc.) from tumor cells obtained from all 10 microdissected DCIS using a small scale RNA extraction protocol (9). Total RNA was similarly extracted from six 20- μ m frozen sections from each of the 28 DCIS tumors constituting the second cohort.

Cell Line Culture and RNA Extraction. The T47D human breast cancer cell line was obtained from the Imperial Cancer Research Fund cell service and grown in DMEM, RPMI or Hams F-12 supplemented with 10% FCS (Globepharm), L-glutamine (2 μ M), penicillin (50 IU/ml), and streptomycin sulfate (50 μ g/ml). Parallel incubations were performed on

flasks of cells approaching confluence in normoxia (humidified air with 5% CO₂) or hypoxia. Hypoxic conditions were generated in a Napco 7001 incubator (Precision Scientific) with 0.1% O₂, 5% CO₂, and balance N₂. Total RNA was prepared according to Chomczynski and Sacchi (14), and the quality assessed by absorbance at 260/280 nm as well as by electrophoresis in 1% agarose gels by staining of the 28S rRNA with ethidium bromide.

Microarray cDNA Membranes. Human GF-200 cDNA Microarray membranes and the Pathways 3.0 analysis software were purchased from Research Genetics, Inc. Reverse transcription, ³³P-labeling, and hybridization of RNA to array membranes were done according to the manufacturer's instructions. Briefly, for each sample, 1 µg of total RNA was reverse transcribed in the presence of 10 µl of [³³P]dCTP at a concentration of 10 mCi/ml, dATP, dGTP, dTTP at 20 mM, 500 ng of oligodeoxythymidylic acid, and 200 units of SuperScript II Reverse Transcriptase (Life Technologies, Inc.), all in a 30-µl volume. The labeled cDNA was purified by passing through a Bio-Spin 6 Chromatography column (Bio-Rad), denatured, and hybridized to human GF-200 cDNA microarray membranes. Membranes were prehybridized at 42°C for at least 2 h in 5 ml of microhyb solution (Research Genetics, Inc.) in the presence of 1.0 µg/ml poly-dA and 1.0 µg/ml Cot 1 DNA. After an overnight (20 h) hybridization with labeled cDNA, membranes were washed, exposed to Imaging screen-K (Bio-Rad), and scanned in a phosphorimager (Bio-Rad), after which they were stripped and reused three times. The tiff images (Fig. 3) obtained from the phosphorimager were imported into the Pathways 3.0 analysis software (Research Genetics, Inc.) for analysis and comparison. The six images from membranes to which ³³P-labeled reverse transcribed RNA from DCIS^{necrosis+} was hybridized were compared with the four images from membranes to which ³³P-labeled reverse transcribed RNA from DCIS^{necrosis-} was hybridized. To compare the two groups of images, an all-data-point method of normalization was used, and cDNAs showing mean expression levels that were statistically different at a confidence level of 75% (Chen test applied by the Pathways 3.0 software) between the two groups of membranes and with ≥ 1.5 differential expression were selected. Each cDNA spot on the Pathways pseudocolor membrane that met the above criteria was examined by direct visualization to eliminate those that might be false positives, spots influenced by bleed over from adjacent spots. A similar approach was used to compare profiles of gene expression between normoxic and hypoxic T47D breast cells.

Real-Time Quantitative RT-PCR. Total RNA from the 10 microdissected samples used for the GeneFilter hybridization and the 28 DCIS samples of the second cohort were reverse transcribed in a total volume of 20 µl as described previously (9). For each sample, 2 µl of 0.1 µg/µl total RNA were added to an 18-µl RT mix (4 µl of 5× RT buffer; 1 µl each of dATP, dCTP, dGTP, and dTTP, all at a concentration of 2.5 mM; 2 µl of 0.1% BSA; 2 µl of 100 mM DTT; 2 µl of DMSO; 2 µl of 50 µM oligodeoxythymidylic acid primer, and 2 µl of 200 units/µl of Moloney murine leukemia virus reverse transcriptase) and incubated at 37°C for 1.5 h. The resulting cDNA was diluted with 20 µl of sterile water and used as template for the quantitative RT-PCR.

The mRNA sequences of the genes identified using the array membranes and corresponding Research Genetics information were determined by using the blast module of National Center for Biotechnology Information database. Primers that specifically detect these sequences were designed and used for the RT-PCR reaction using the LightCycler Instrument (Roche Molecular Biochemicals) and the LightCycler-DNA Master Sybr Green I reaction mix for PCR (Roche Molecular Biochemicals), containing the Sybr Green I dye as detection format. For each sample, triplicate reactions were set up in capillaries with the following reaction mix: 0.33 µl of DNA template; 0.2 µl each of 50 mM sense and antisense primers; 1.6 µl of 25 mM MgCl₂; 2 µl of LightCycler-DNA Master Sybr Green I reaction mix; and 16 µl sterile water. For each batch of reactions, controls included RT-negative and RNA-negative controls and serial dilutions (1, 0.01, and 0.0001 ng) of plasmid DNA as standards for linear regression analysis of unknown samples. The denaturation, amplification, melting curve analysis, and cooling programs of the LightCycler instrument were set according to manufacturer's specifications. The annealing temperature and elongation time, however, were set depending on primers and product length, respectively. PCR products were run on a 1.5% agarose gel to confirm the PCR specificity. The expression of cyclophilin 33A, a house keeping gene, was used to normalize for variances in RNA and cDNA input. The AAMP primers were sense, 5'-CGCCTGCTTACTGACTACC-3', and antisense, 5'-GTATCTCTCCTCCTTCCAC-3', with annealing temperature of 57°C and elongation time of 20 s. The NDR serine threonine protein kinase primers were sense, 5'-TTG CAC AGG ACT GAA AAA-3', and antisense, 5'-ATACAAA-GAACTCTGCTCCAC-3', with annealing temperature of 60°C and elongation time of 50 s. The cyclophilin 33A primers were sense, 5'-GCTGCCGTTTCATTCTTTG-3', and antisense, 5'-CTCCTGGGTCTGCTTTG-3', with annealing temperature of 60°C and elongation time of 10 s.

ISH. Paraffin-embedded 5-µm breast tumor sections were analyzed for AAMP mRNA expression by ISH, according to a previously described protocol (15). The plasmid pT7T3D-pac containing a 460-bp insert of the human AAMP cDNA (Image consortium clone Id 789011, GenBank accession no. AA452988) was used as a template to generate sense and antisense probes. UTP ³⁵S-labeled riboprobes were synthesized using Riboprobe Systems (Promega, Madison, WI) according to manufacturer's instructions. Sense probes were used as controls. ISH and washing conditions were as described previously (15). Sections were developed, after 5 weeks, using Kodak NTB-2 photographic emulsion and counterstained with Lee's stain (15).

Levels of AAMP mRNA expression were assessed in the sections by microscopic examination using a semiquantitative approach (15). Scores were obtained by estimating the average signal (on a scale of 0–3) and the proportion of ductal cells showing a positive signal (0, none; 0.1, <10%; 0.5, <50%; 1.0, >50%). The intensity and proportion score were then multiplied to give an overall score.

Statistics. The Mann-Whitney *U* test, the Fisher's exact test, and the Pearson's correlation were used as appropriate. To determine the reproducibility of hybridization results with the GF-200 membrane, the normalized intensity values of all of the 5544 gene spots from duplicate hybridizations of duplicate

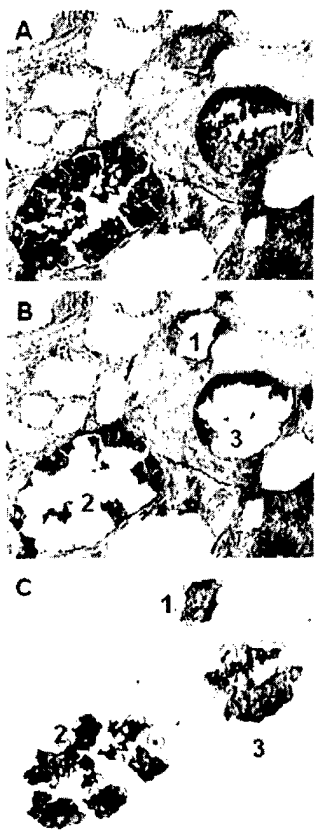


Fig. 1. LCM of duct cells from H&E-stained frozen section (10 μ m) of a high-grade DCIS of the breast. A, three ducts (1, 2, and 3) identified for dissection. B, ducts after dissection. C, cells from duct successfully captured and transferred.

33 P-labeled cDNA of RNA sample from the T47D cell line, one hybridization was to a fresh membrane and the other to a stripped membrane, were compared by linear regression and correlation analyses. For all tests, statistical significance was considered to be at the $P < 0.05$ level (Graphpad prism; Graphpad Software, San Diego, CA).

RESULTS

Microdissection and Microarray cDNA Filters. The manual and laser-assisted microdissection techniques proved to be equally effective in isolating ductal carcinoma cells from our DCIS specimens (Fig. 1). We were able to isolate ~ 2 μ g of total RNA from 14 to 17 10- μ m frozen sections of the two tumors subjected to the laser-assisted method of dissection, whereas the manual dissection method yielded ~ 2 –4 μ g of total RNA from 6 to 10 20- μ m frozen sections of tumor samples. The quality of hybridization signals produced by the labeled reverse transcribed total RNA obtained by both dissection techniques were also comparable as assessed by the exposure time needed to obtain equivalent signal intensities for analysis.

We compared the 6 DCIS with necrosis to the 4 DCIS without necrosis using the Pathways 3.0 software. The Chen and

t tests were applied using the Pathways 3.0 software (at a confidence level of 75%) to filter out cDNA pairs (4363 or 78% of the 5544 transcripts represented on the membrane), the mean intensities of which were not statistically different. Of the remaining 1181 transcripts, we masked those with intensities <5 \times background and excluded false positives, spots judged to be influenced by bleed over, from adjacent spots. After this filtering process, 69 transcripts remained that were ≥ 1.5 -fold differentially expressed between the 6 DCIS^{necrosis+} and 4 DCIS^{necrosis-}. Fifty-two of the transcripts were overexpressed by the DCIS^{necrosis+} group, and 17 transcripts were overexpressed by the DCIS^{necrosis-} group. Pearson correlation test showed that there was a greater degree of similarity in the expression of these 69 transcripts when tumors were compared within the DCIS^{necrosis-} group ($r = 0.94$ –0.96) than when tumors were compared within the DCIS^{necrosis+} group of tumors, among which expression was more variable ($r = 0.70$ –0.99). To identify genes that were both differentially expressed and that also might be associated with hypoxia, we compared the set of 52 cDNAs consistently overexpressed in DCIS^{necrosis+} (Table 2) with 22 cDNAs found to be overexpressed in the T47D cell line subjected to hypoxia when this was analyzed in parallel with the DCIS lesions using the same microarray filter. Two genes, AAMP and NDR, were found to be common to both sets of differentially expressed genes and, when retested by *t* test, were significantly different between the two groups of DCIS at the 99% confidence level, and these were assessed further.

Real-Time Quantitative RT-PCR for AAMP and NDR mRNA. AAMP and NDR mRNA expression levels were assessed by RT-PCR in the 10 original microdissected tumors. AAMP and NDR expression levels in the microdissected ductal epithelium from the initial 10 DCIS tumors were higher in DCIS^{necrosis+} compared with the DCIS^{necrosis-} group, but only AAMP expression was significantly different ($P = 0.0095$; Mann-Whitney, two tailed) between the two groups (Fig. 2). To examine AAMP expression further, we studied 28 additional nonmicrodissected DCIS samples. RT-PCR assay in one sample from this second DCIS cohort failed to yield a product with the control. Among the remaining 27 nonmicrodissected DCIS series, total AAMP expression within the tumor section was associated with higher grade and necrosis ($P = 0.0427$; Mann-Whitney, one-tailed; Fig. 2B). The overall expression level of AAMP in these 27 tumors did not show any association with either the PR ($P = 0.55$; Mann-Whitney) or ER ($P = 0.37$; Mann-Whitney) status of the tumors.

ISH. AAMP mRNA expression was also assessed by ISH in all 37 tumors. The AAMP antisense probe showed stronger signals for AAMP mRNA in high-grade DCIS ducts and DCIS ducts with necrosis as compared with low-grade ducts, with variation from duct to duct in individual tumors. However there was no marked gradation in expression from luminal to stromal aspect of ducts with central necrosis. Expression was also observed in blood vessels in the stroma around the ducts (Fig. 3). The ISH intensity score assigned to each tumor was based on an average of the epithelial expression assessed from all of the ducts in the sections examined. AAMP expression detected by ISH showed a relationship to grade and necrosis, although this association was at best of borderline signifi-

Table 2 Sixty-nine transcripts that were differentially expressed between the DCIS^{necrosis+} and DCIS^{necrosis-} lesions

Serial number	Accession no.	Gene symbol	Fold change
1	R44202	COMT	9.8
2	W39343	RALB	5.1
3	R25074	EST	3.5
4	N90968	EST	3.2
5	AA428778	EFNB1	2.8
6	T69485	EST	2.7
7	H94236	EST	2.6
8	H70114	EST	2.5
9	R15709	EST	2.5
10	H75699	KIAA0329	2.5
11	R91904	AQP3	2.3
12	H46663	PURA	2.2
13	T70098	SLC1A5	2.2
14	AA040424	dA141HS.1	2.1
15	H73724	CDK6	2.1
16	H77479	EST	2.1
17	AA100612	RBM10	2.1
18	AA486082	SGK	2.1
19	H25229	DKFZP434D1335	2.1
20	W01211	EST	2.1
21	H58040	EST	2
22	AA488233	PRCC	1.9
23	H58949	EST	1.9
24	AA521346	NDR	1.9
25	AA115901	CRTL1	1.9
26	N51018	BGN	1.9
27	AA521083	PPP6C	1.8
28	W52208	COTL1	1.8
29	H65066	VSNL1	1.8
30	AA034501	EST	1.7
31	AA479623	SAST	1.7
32	N76581	KIAA0130	1.7
33	H23187	CA2	1.7
34	W72813	EST	1.7
35	H08749	MAP2K3	1.6
36	AA074677	EST	1.6
37	AA490684	AEB1	1.6
38	AA487197	UBE2I	1.6
39	AA451969	TCEAL1	1.6
40	T67053	IGL@	1.6
41	AA070997	PSMB6	1.6
42	AA598508	CRABP2	1.6
43	AA485653	MGAT2	1.5
44	AA490991	HNRNPF	1.5
45	AA452988	AAMP	1.5
46	AA136359	CD58	1.5
47	R27585	PSMA1	1.5
48	AA463492	CYBB	1.5
49	N90470	EST	1.5
50	AA461231	TSN	1.5
51	AA608557	DDB1	1.5
52	AA403083	PSEN1	1.5
53	AA456931	COXC6	2.2
54	R51346	METAP2	2.2
55	R36571	EST	2.1
56	R40212	COPA	2.1
57	R64153	EST	1.7
58	N95112	RNF3	1.6
59	R36624	EST	1.6
60	N72313	EST	1.5
61	R40460	PIK4CA	1.5
62	N54596	IGF2	1.5
63	N90335	C21ORF4	1.5
64	R38459	EST	1.5
65	H28710	EDNRB	1.5
66	R76365	PLCG1	1.5
67	R52548	SOD1	1.5
68	T66907	EST	1.5
69	AA402960	RNF5	1.5

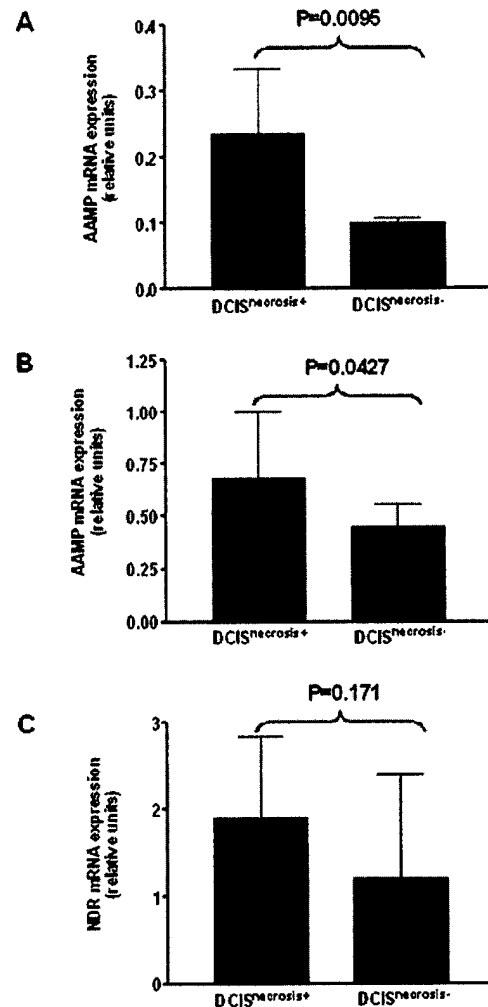


Fig. 2 A, AAMP mRNA expression detected by RT-PCR shown relative to grade and necrosis in 10 microdissected DCIS samples ($n = 6$ DCIS^{necrosis+}, $n = 4$ DCIS^{necrosis-}). B, AAMP mRNA expression detected by RT-PCR shown relative to grade and necrosis in 27 DCIS of the breast ($n = 21$ DCIS^{necrosis+}, $n = 6$ DCIS^{necrosis-}). C, NDR mRNA expression in the same samples as in A, showing higher expression in DCIS^{necrosis+} compared with DCIS^{necrosis-} but not to a statistically significant level.

cance. AAMP ISH scores were higher in high and intermediate grade DCIS ($P = 0.05$; Fisher's exact test) and in tumors with necrosis ($P = 0.09$; Fisher's exact test) compared with low grade and those without necrosis, respectively. There was no association between the levels of AAMP detected by ISH and the ER ($P = 0.2$; Fisher's exact test) or PR ($P = 0.5$; Fisher's exact test) status of tumors.

DISCUSSION

We have shown that although levels of gene expression are mostly similar between morphologically different DCIS, consistent differences in expression of a subset of genes can be identified between low-grade and high-grade DCIS. Among

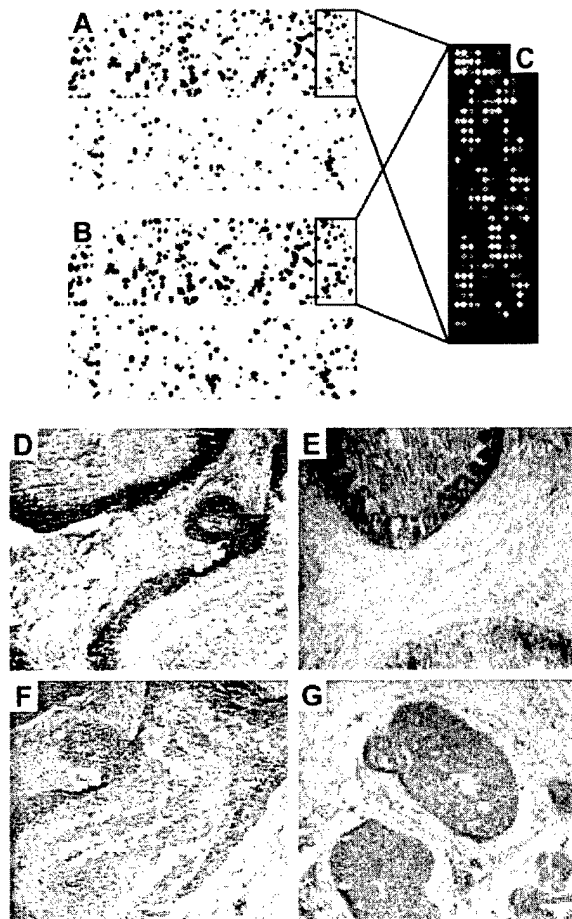


Fig. 3 Differential gene expression analysis using the GF200 cDNA array membrane and the Pathways 3.0 analysis software and confirmation of differential expression of AAMP by ISH. *A–C* show human GF200 cDNA array membranes after hybridization of ^{33}P -labeled reverse transcribed RNA from a DCIS $^{\text{necrosis}+}$ (*A*) and a DCIS $^{\text{necrosis}-}$ (*B*) and a portion of a software-generated synfilter representation of differential gene expression between these two DCIS $^{\text{necrosis}+}$ and DCIS $^{\text{necrosis}-}$ lesions. AAMP is represented by the *spot* surrounded by a *rectangle*. *D–G* show ISH with ^{35}S -labeled antisense probe for AAMP and demonstrate strong signals for AAMP in high-grade ducts with necrosis (*D* and *E*), weaker signals in a DCIS $^{\text{necrosis}-}$ lesion (*G*), and absence of signal with the sense probe (*F*), $\times 40$ original magnification.

these differentially expressed genes, the AAMP was found to be expressed at a higher level by most high-grade DCIS and DCIS with necrosis and is also overexpressed in a breast cancer cell line subjected to hypoxia.

The two microdissection techniques used in this study were effective in isolating ductal cells from our samples. The laser-assisted microdissection, however, limits the thickness of sections for dissection to a maximum of 10 μm , hence the need to dissect more sections to obtain a reasonable yield of RNA for hybridization. An alternate approach would be to dissect a minimum number of cells to obtain enough RNA that could serve as a template for transcriptional-based RNA amplification (16). Our approach of dissecting cells from several sections,

although seemingly burdensome, avoids the technical difficulties associated with RNA amplification.

cDNA microarray analysis is a powerful tool for the simultaneous analysis of large sets of genes and for the profiling of different tissue types. Studies have, however, shown that any single microarray output is subject to some variability and that pooling of data from replicates can provide a more reliable classification of gene expression (17). In this study, the small amount of RNA available from some of our microdissected samples precluded us from carrying out replicate array experiments on the same sample. We have, however, attempted to address the issue of variability by pooling data from different tumors. This we believe may be more stringent than replicate experiments on the same sample. In addition, the 75% confidence level applied to filter the cDNA pairs, although seemingly lax, allowed us to identify those transcripts that were differentially expressed between the DCIS $^{\text{necrosis}-}$ lesions and any three or more of the six DCIS $^{\text{necrosis}+}$ tumors. The variability in the expression of the 69 transcripts among the DCIS $^{\text{necrosis}+}$ may be accounted for by the different proportion of ducts with the presence of necrosis among this group (25–75%).

We are not aware of another study with comparable expression profiling data to compare different grades of DCIS. However, similar to our findings, studies based on techniques that can use paraffin block material (DNA-based loss of heterozygosity/allelic imbalance studies as well as comparative genomic hybridization studies) have shown that there are distinct genetic changes associated with the level of differentiation/grade and morphology of DCIS of the breast (18–20).

Among the genes overexpressed by DCIS $^{\text{necrosis}+}$ tumors (Table 2), the kinases, *NDR* and *SGK*, and the phosphatase, *PPP6C*, are serine/threonine specific in their catalytic activities, and they have been implicated in cell cycle regulation (21–23). In addition, *NDR* and *PPP6C* regulate cell morphology (22, 23), whereas *SGK* is able to prevent the fork head transcription factor-induced apoptosis (24). Furthermore, *NDR* kinase is regulated by calcium and is mediated by the S-100 calcium-binding proteins (25). A member of the S100 calcium-binding protein family, *S100A7* (psoriasin), is differentially expressed in DCIS lesions compared with invasive tumors (26). Whether there is any relationship between the expression of *NDR* and any of the S100 protein family of genes in DCIS lesions remains to be assessed. *UBE2I*, the human homologue of the yeast *UBC9* that mediates the transition from G₁ to S phase of the cell cycle (27), is proposed to interact with *RAD51* and *RAD52*, which are part of the *BRCA1* pathway (28, 29) as well as with *TP53* (28). *PRCC*, the translocation gene in papillary renal cell carcinoma is speculated to function in the signaling cascade because it possesses a proline-rich domain (30). Its recent association with graft-versus-host reaction (31) raises the possibility that it might play a role in inflammatory response that is frequently associated with high-grade comedo type DCIS. *CA II*, a cytosolic CA isoenzyme, is highly expressed in several tumor types, including gastric, colorectal, and pancreatic carcinomas (32–34) as well as malignant brain tumors (35), and its expression has been shown to correlate with biological aggressiveness of rectal cancer (34). Furthermore, we have recently found that altered expression of other CAs, *CA IX* and *CAXII*, is a frequent occurrence between low- and high-grade DCIS (12). The expression of these trans-

membrane isoenzymes is influenced by hypoxia and differentiation, and they are expressed on different aspects of the breast cell membrane where they may act to influence the local extracellular pH surrounding the cancer cells, thereby possibly creating a microenvironment conducive for tumor growth and spread (36). In preliminary experiments, we have not been able to demonstrate hypoxia regulation of *CA II* in breast cell lines (data not shown) and a similar role for the intracellular *CA II* in the progression of breast cancer remains to be determined. However, higher levels of the intracellular *CA II* in high-grade DCIS may be part of coordinated changes in pH regulation, and by causing an increased generation of intracellular CO₂, *CA II* may facilitate the actions of the extracellular CA isoenzymes (37).

Solute carrier family 1, member 5 (neutral amino acid transporter; *SLC1A5*) was reported to show elevated levels of expression in multicellular hepatoma spheroids displaying central necrosis, similar to that seen in high-grade DCIS when compared with single cell suspension. This elevated level of *SLC1A5* mRNA paralleled changes in glutamine uptake by tumor cells in this model, suggesting that a hypoxic tumor microenvironment impacts on the uptake of specific nutrients (38). Because one important goal of expression profiling is to develop a molecular-based classification system for tumors (39, 40), additional expression-profiling studies of a larger series of DCIS of the breast would be necessary to give insight into the importance of these genes in developing a molecular signature for DCIS of the breast.

AAMP was first isolated from a human melanoma cell line as a motility-associated cell protein and was found to be expressed strongly in endothelial cells, cytotrophoblast, and poorly differentiated colon adenocarcinoma cells found in lymphatics (41). In addition, gene expression studies have shown that AAMP is overexpressed by gastrointestinal stromal tumors (42). AAMP has two immunoglobulin domains and six WD40 repeat domains, suggesting possible membership in both the immunoglobulin superfamily and the WD40 repeat family of proteins (43, 44). The presence of both the immunoglobulin-type domains and WD40 repeats sequence motifs in AAMP implies a multifunctional role for this protein (44). Experimental evidence to date suggests that AAMP may play a role in cell motility and angiogenesis. This has been examined and demonstrated in endothelial cells (45). However, we and others have shown that AAMP is expressed by other cells and this property, which may be related to the fact that it shares a common epitope with α -actinin and a fast twitch skeletal muscle fiber protein (43), is not necessarily restricted to endothelial cells and angiogenesis (45). However, this extraepithelial source of AAMP would probably account for the inability to fully reproduce the AAMP-grade/necrosis association demonstrated in our microdissected series in the nonmicrodissected cohort, underscoring the usefulness of microdissection techniques in profiling ubiquitously expressed genes from specific cell types in a heterogeneous tissue environment.

Necrosis is believed to represent the extreme manifestation of hypoxia in tissues (46). The finding that AAMP is induced *in vitro* in a breast cell line subjected to hypoxia and also *in vivo* in DCIS associated with necrosis suggest that AAMP may be a hypoxia-regulated gene that may influence growth and survival

of DCIS. However, necrosis may be attributable to other causes and alternative stresses may influence gene expression in cells subjected to hypoxia (47). Regulation by hypoxia *in vitro* may also not be the only or dominant factor in the complex *in vivo* environment (12). Additional work will be required to establish if AAMP expression is directly regulated by mediators of hypoxia response *in vivo*.

In summary, we have shown that DCIS with necrosis can be distinguished from DCIS without necrosis by the pattern of gene expression and that up-regulation of AAMP, a gene that has previously been associated with angiogenesis and tumor progression, is also associated with a high nuclear grade morphology and necrosis in DCIS of the breast.

REFERENCES

1. Ernst, V. L., and Barclay, J. Increase in ductal carcinoma *in situ* (DCIS) of breast in relation to mammography: a dilemma. *J. Natl. Cancer Inst. Monogr.*, 22: 151–156, 1997.
2. Elston, C. W., Ellis, I. O., and Pinder, S. E. Prognostic factors in invasive carcinoma of the breast. *Clin. Oncol. (R. Coll. Radiol.)*, 10: 14–17, 1998.
3. Silverstein, M. J., Lagios, M. D., Craig, P. H., Waisman, J. R., Lewinsky, B. S., Colburn, W. J., and Poller, D. N. A prognostic index for ductal carcinoma *in situ* of the breast. *Cancer (Phila.)*, 77: 2267–2274, 1996.
4. Sneige, N., Lagios, M. D., Schwarting, R., Colburn, W., Atkinson, E., Weber, D., Sahn, A., Kemp, B., Hoque, A., Risin, S., Sabichi, A., Boone, C., Dhingra, K., Kelloff, G., and Lippman, S. Interobserver reproducibility of the Lagios nuclear grading system for ductal carcinoma *in situ*. *Hum. Pathol.*, 30: 257–262, 1999.
5. Lagios M. D. Duct carcinoma *in situ*: biological implications for clinical practice. *Semin. Oncol.*, 23 (1 Suppl. 2): 6–11, 1996.
6. Sakorafas, G. H., and Tsiotou, A. G. H. Ductal carcinoma *in situ* (DCIS) of the breast: evolving perspectives. *Cancer Treat. Rev.*, 26: 103–125, 2000.
7. Winchester, D. P., and Strom, E. A. Standards for diagnosis and management of ductal carcinoma *in situ* (DCIS) of the breast. *CA - Cancer J. Clin.*, 48: 108–128, 1998.
8. Watson, P., Snell, L., and Parisien, M. The role of a tumor bank in translational research. *Can. Med. Assoc. J.*, 15: 281–283, 1996.
9. Hiller, T., Snell, L., and Watson, P. H. An approach for microdissection/RT-PCR analysis of gene expression in pathologically defined frozen tissue sections. *Biotechniques*, 21: 38–42, 1996.
10. Luzzi, V., Holtschlag, V., and Watson, M. A. Expression profiling of ductal carcinoma *in situ* by laser capture microdissection and high-density oligonucleotide arrays. *Am. J. Pathol.*, 158: 2005–2010, 2001.
11. Fisher, E. R., Dignam, J., Tan-Chiu, E., Costantino, J., Fisher, B., Paik, S., and Wolmark, N. Pathologic findings from the National Surgical Adjuvant Breast Project (NSABP) eight-year update of Protocol B-17: intraductal carcinoma. *Cancer (Phila.)*, 86: 429–438, 1999.
12. Wykoff, C. C., Beasley, N., Watson, P. H., Campo, L., Chia, S. K., English, R., Pastorek, J., Sly, W. S., Ratcliffe, P., and Harris, A. L. Expression of hypoxia-inducible and tumor-associated carbonic anhydrase in ductal carcinoma *in situ* of the breast. *Am. J. Pathol.*, 158: 1011–1019, 2001.
13. Silverstein, M. J., Poller, D. N., Waisman, J. R., Colburn, W. J., Barth, A., Gierson, E. D., Lewinsky, B., Gamagani, P., and Slamon, D. J. Prognostic classification of breast ductal carcinoma-*in-situ*. *Lancet*, 345: 1154–1157, 1995.
14. Chomczynski, P., and Sacchi, N. Single-step method of RNA isolation by acid guanidinium thiocyanate-phenol-chloroform extraction. *Anal. Biochem.*, 162: 156–159, 1987.
15. Leygue, E., Snell, L., Dotzlaw, H., Hole, K., Troup, S., Hiller-Hitchcock, T., Murphy, L. C., and Watson, P. H. Mammoglobin, a

potential marker of breast cancer nodal metastasis. *J. Pathol.*, **189**: 28–33, 1999.

16. Sgroi, D. C., Teng, S., Robinson, G., LeVangie, R., Hudson, J. R., and Elkaloun, A. G. *In vivo* gene expression profile analysis of human breast cancer progression. *Cancer Res.*, **59**: 5656–5661, 1999.
17. Lee, M. L. T., Kuo, F. C., Whitmore, G. A., and Sklar, J. Importance of replication in microarray gene expression studies: statistical methods and evidence from repetitive cDNA hybridizations. *Proc. Natl. Acad. Sci. USA*, **97**: 9834–9839, 2000.
18. O'Connell, P., Pekkel, V., Fuqua, S. A. W., Osborne, K., Clark, G., and Allred, D. C. Analysis of loss of heterozygosity in 399 premalignant breast lesions at 15 genetic loci. *J. Natl. Cancer Inst. (Bethesda)*, **90**: 697–703, 1998.
19. Ando, Y., Iwase, H., Ichihara, S., Toyoshima, S., Nakamura, T., Yamashita, H., Toyama, T., Omoto, Y., Karamatsu, S., Mitsuyama, S., Fujii, Y., and Kobayashi, S. Loss of heterozygosity and microsatellite instability in ductal carcinoma *in situ* of the breast. *Cancer Lett.*, **156**: 207–214, 2000.
20. Buerger, H., Otterbach, F., Simon, R., Poremba, C., Diallo, R., Decker, T., Riehdorf, L., Brinkschmidt, C., Dockhorn-Dworniczak, B., and Boecker, W. Comparative genomic hybridization of ductal carcinoma *in situ* of the breast—evidence of multiple genetic pathways. *J. Pathol.*, **187**: 396–402, 1999.
21. Millward, T., Cron, P., and Hemmings, B. A. Molecular cloning and characterization of a conserved nuclear serine/threonine protein kinase. *Proc. Natl. Acad. Sci. USA*, **92**: 5022–5026, 1995.
22. Millward, T. A., Hess, D., and Hemmings, B. A. Ndr protein kinase is regulated by phosphorylation on two conserved sequence motifs. *J. Biol. Chem.*, **274**: 33847–33850, 1999.
23. Bastians, H., and Ponstingl, H. The novel human protein serine/threonine phosphatase 6 is a functional homologue of budding yeast Sit4p and fission yeast ppe1, which are involved in cell cycle regulation. *J. Cell Sci.*, **109**: 2865–2874, 1996.
24. Brunet, A., Park, J., Tran, H., Hu, L. S., Hemmings, B. A., and Greenberg, M. E. Protein kinase SGK mediates survival signals by phosphorylating the forkhead transcription factor FKHL1 (FOXO3a). *Mol. Cell. Biol.*, **21**: 952–965, 2001.
25. Willward, T. A., Heizmann, C. W., Schäfer, B. W., and Hemmings, B. A. Calcium regulation of Ndr protein kinase mediated by S100 calcium binding proteins. *EMBO J.*, **17**: 5913–5922, 1998.
26. Leygue, E., Snell, L., Hiller, T., Dotzlaw, H., Hole, K., Murphy, L. C., and Watson, P. H. Differential expression of psoriasis messenger RNA between *in situ* and invasive human breast carcinoma. *Cancer Res.*, **56**: 4606–4609, 1996.
27. Watanabe, T. K., Fujiwara, T., Kawai, A., Shimizu, F., Takami, S., Hirano, H., Okuno, S., Ozaki, K., Takeda, S., Shimada, Y., Nagata, M., Takaichi, A., Takahashi, E., Nakamura, Y., and Shin, S. Cloning, expression, and mapping of UBE2I, a novel gene encoding a human homologue of yeast ubiquitin-conjugating enzymes which are critical for regulating the cell cycle. *Cytogenet. Cell Genet.*, **72**: 86–89, 1996.
28. Shen, Z., Pardington-Purtyman, P. E., Comeaux, J. C., Moyzis, R. K., and Chen, D. J. Associations of UBE2I with RAD52, UBL1, p53, and RAD51 proteins in a yeast two-hybrid system. *Genomics*, **37**: 183–186, 1996.
29. Welcsh, P. L., Owens, K. N., and King, M. C. Insights into the functions of BRCA1 and BRCA2. *Trends Genet.*, **16**: 69–74, 2000.
30. Weterman, M. J., van Groningen, J. J., Jansen, A., and van Kessel, A. G. Nuclear localization and transactivating capacities of the papillary renal cell carcinoma-associated TFE3 and PRCC (fusion) proteins. *Oncogene*, **19**: 69–74, 2000.
31. Wakui, M., Yamaguchi, A., Sakurai, D., Ogasawara, K., Yokochi, T., Tsuchiya, N., Ikeda, Y., and Tokunaga, K. Genes highly expressed in the early phase of murine graft-versus-host reaction. *Biochem. Biophys. Res. Commun.*, **282**: 200–206, 2001.
32. Parkkila, S., Parkkila, A. K., Juvonen, T., Lehto, V. P., and Rajaniemi, H. Immunohistochemical demonstration of the carbonic anhydrase isoenzymes I and II in pancreatic tumours. *Histochem. J.*, **27**: 133–138, 1995.
33. Pastorekova, S., Parkkila, S., Parkkila, A. K., Opavsky, R., Zelnik, V., Saarnio, J., and Pastorek, J. Carbonic anhydrase IX, MN/CA IX: analysis of stomach complementary DNA sequence and expression in human and rat alimentary tracts. *Gastroenterology*, **112**: 398–408, 1997.
34. Bekku, S., Mochizuki, H., Yamamoto, T., Ueno, H., Takayama, E., and Tadakuma, T. Expression of carbonic anhydrase I or II and correlation to clinical aspects of colorectal cancer. *Hepatogastroenterology*, **47**: 998–1001, 2000.
35. Parkkila, A. K., Herva, R., Parkkila, S., and Rajaniemi, H. Immunohistochemical demonstration of human carbonic anhydrase isoenzyme II in brain tumours. *Histochem. J.*, **27**: 974–982, 1995.
36. Ivanov, S. V., Kuzmin, I., Wei, M. H., Pack, S., Geil, L., Johnson, B. E., Stanbridge, E. J., and Lerman, M. I. Down-regulation of transmembrane carbonic anhydrases in renal cell carcinoma cell lines by wild-type von Hippel-Lindau transgenes. *Proc. Natl. Acad. Sci. USA*, **95**: 12596–12601, 1998.
37. Parkkila, S., Rajaniemi, H., Parkkila, A. K., Kivela, J., Waheed, A., Pastorekova, S., Pastorek, J., and Sly, W. S. Carbonic anhydrase inhibitor suppresses invasion of renal cancer cells *in vitro*. *Proc. Natl. Acad. Sci. USA*, **97**: 2220–2224, 2000.
38. Pawlik, T. M., Souba, W. W., Sweeney, T. J., and Bode, B. P. Amino acid uptake and regulation in multicellular hepatoma spheroids. *J. Surg. Res.*, **9**: 15–25, 2000.
39. Perou, C. M., Jeffrey, S. S., van de Rijn, M., Rees, C. A., Eisen, M. B., Ross, D. T., Pergamenschikov, A., Williams, C. F., Zhu, S. X., Lee, J. C., Lashkari, D., Shalon, D., Brown, P. O., and Botstein, D. Distinctive gene expression patterns in human mammary epithelial cells and breast cancers. *Proc. Natl. Acad. Sci. USA*, **96**: 9212–9217, 1999.
40. Perou, C. M., Sorlie, T., Eisen, M. B., van de Rijn, M., Jeffrey, S. S., Rees, C. A., Pollack, J. R., Ross, D. T., Johnsen, H., Akslen, L. A., Fluge, O., Pergamenschikov, A., Williams, C., Zhu, S. X., Lonning, P. E., Borresen-Dale, A. L., Brown, P. O., and Botstein, D. Molecular portraits of human breast tumours. *Nature (Lond.)*, **406**: 747–752, 2000.
41. Beckner, M. E., Krutzsch, H. C., Stracke, M. L., Williams, S. T., Gallardo, J. A., and Liotta, L. A. Identification of a new immunoglobulin superfamily protein expressed in blood vessels with a heparin-binding consensus sequence. *Cancer Res.*, **55**: 2140–2149, 1995.
42. Allander, S. V., Nupponen, N. N., Ringner, M., Hostetter, G., Maher, G. W., Goldberger, N., Chen, Y., Carpten, J., Elkahloun, A. G., and Meltzer, P. S. Gastrointestinal stromal tumors with KIT mutations exhibit a remarkably homogeneous gene expression profile. *Cancer Res.*, **61**: 8624–8628, 2001.
43. Beckner, M. E., Krutzsch, H. C., Klipstein, S., Williams, S. T., Maguire, J. E., Doval, M., and Liotta, L. A. AAMP, a newly identified protein, shares a common epitope with α -actinin and a fast skeletal muscle fibre protein. *Exp. Cell Res.*, **225**: 306–314, 1996.
44. Beckner, M. E., and Liotta, L. A. AAMP, a conserved protein with immunoglobulin and WD40 domains, regulates endothelial tube formation *in vitro*. *Lab. Investig.*, **75**: 97–107, 1996.
45. Beckner, M. E., Peterson, V. A., and Moul, D. E. Angio-associated migratory protein is expressed as an extracellular protein by blood-vessel-associated mesenchymal cells. *Microvasc. Res.*, **57**: 347–352, 1999.
46. Leek, R. D., Landers, R. J., Harris, A. L., and Lewis, C. E. Necrosis correlates with high vascular density and focal macrophage infiltration in invasive carcinoma of the breast. *Br. J. Cancer*, **79**: 991–995, 1999.
47. Bos, R., Zhong, H., Hanrahan, C. F., Mommers, E. C., Semenza, G. L., Pinedo, H. M., Abeloff, M. D., Simons, J. W., van Diest, P. J., and van der Wall, E. Levels of hypoxia-inducible factor-1 α during breast carcinogenesis. *J. Natl. Cancer Inst. (Bethesda)*, **93**: 309–314, 2001.